Ground State and Excited Stated Properties of Hexaamminechromium(III) Ion: A Density Functional Study

Karel Doclo, David De Corte, and Claude Daul*

Institut de Chimie Inorganique et Analytique, University of Fribourg, CH 1700 Fribourg, Switzerland

Hans-Ueli Güdel

Department of Chemistry, University of Bern, CH 3000 Bern, Switzerland

Received December 4, 1997

The electronic structure of the ground and lowest excited states of the hexaamminechromium(III) ion $[Cr(NH_3)_6]^{3+}$ has been investigated through density functional theory. The geometry of the $^4A_{2g}$ ground state and of the $^4T_{2g}$ excited state are optimized. The latter is relaxed along an e_g Jahn−Teller coordinate. The experimentally known geometry distortion, i.e., an axial compression and an equatorial elongation, together with the corresponding energy gain is well reproduced by our calculations. The results for the d−d excitation energies are in reasonable agreement with experiment. The relative performance of local and gradient-corrected functionals is discussed.

1. Introduction

The photochemistry of chromium(III) ammine complexes has been widely studied experimentally. This abundant amount of data and the empirical rules of Adamson[1] have led to theoretical models for understanding the observed photochemistry. In this respect, the approach of Zink,[2−5] based on the ligand field model, and especially that of Vanquickenborne et al.,[6−9] using the angular overlap model, are very useful. However, only few first-principle studies[10,11] have been devoted to the chromium(III) ammine compounds, and to our knowledge, this is the first study where also the geometrical parameters of $[Cr(NH_3)_6]^{3+}$ are derived from first principles.

Cr^{3+} has a large preference for octahedral symmetry. In the absorption spectra at room temperature one sees in general broad bands, consisting of spin-allowed quartet absorptions, and narrow bands, arising from spin-forbidden doublet transitions. In the chromium(III) ammine complexes, the ^2E_g state is the first excited sate, but the $^4T_{2g}$ state can become thermally accessible at room temperature. Different paths for the photoreaction can thus be proposed:[12−15] (1) a prompt reaction from the $^4T_{2g}$ state; (2) a direct reaction from the doublet state ^2E_g to the final product(s) without back intersystem crossing (bisc); (3) doublet state deactivation via a thermally activated bisc process; (4) reaction from the doublet state to a ground state intermediate.

A relevant issue in understanding the photochemistry is the knowledge of the relative positions of the potential energy surfaces of the ground and excited states, since the important excited states appear to be the so-called thexi states (that is, the states reached after thermal equilibration) rather than the Franck−Condon states. Experimentally, the geometry of the ground state is obtained through X-ray analysis. Information about the geometry of the excited states can be extracted from absorption and emission spectra. Vibrational frequencies reflect the shape of the potential energy surfaces. $[Cr(NH_3)_6]^{3+}$ is one of the few complexes where very detailed information on the potential energy surfaces could be obtained through high-resolution solid state absorption spectroscopy at very low temperature.[16] The ^2E_g excited state has the same geometry as the $^4A_{2g}$ ground state, but the $^4T_{2g}$ excited state couples to both the a_{1g} and, in a dynamical Jahn−Teller effect, the e_g vibration of the $[Cr(NH_3)_6]^{3+}$ octahedron. This results in a distorted geometry relative to the $^4A_{2g}$ ground state, i.e., an expansion of 0.12 Å of the Cr−N bond length along two axes and a contraction of 0.02 Å along the third axis are observed. Solomon et al.[16] have proposed this Jahn−Teller distortion as a possible factor for subsequent substitution steps. Thus, $[Cr(NH_3)_6]^{3+}$ turns out to be an ideal test case to probe the ability of density functional (DF) theory to describe both ground state (GS) and excited state (ES) properties. We investigated the GS geometry and the multiplet structure arising from intraconfigurational quartet−doublet transitions and interconfigurational quartet−quartet transitions. A very important point is to check whether the experimentally observed Jahn−Teller distortion of the $^4T_{2g}$ state can be reproduced. If this is the case, DF

(1) Adamson, A. W. *J. Phys. Chem.* **1967**, *71*, 798.
(2) Zink, J. I. *J. Am. Chem. Soc.* **1972**, *94*, 8039.
(3) Zink, J. I. *Inorg. Chem.* **1973**, *12*, 1957.
(4) Zink, J. I. *J. Am. Chem. Soc.* **1974**, *96*, 4464.
(5) Zink, J. I. *Inorg. Chem.* **1975**, *14*, 446.
(6) Vanquickenborne, L. G.; Ceulemans, A. *J. Am. Chem. Soc.* **1977**, *99*, 2208.
(7) Vanquickenborne, L. G.; Ceulemans, A. *J. Am. Chem. Soc.* **1978**, *100*, 475.
(8) Vanquickenborne, L. G.; Ceulemans, A. *Inorg. Chem.* **1979**, *18*, 3475.
(9) Vanquickenborne, L. G.; Ceulemans, A. *Coord. Chem. Rev.* **1983**, *48*, 175.
(10) Vanquickenborne, L. G.; Coussens, B.; Postelmans, D.; Ceulemans, A.; Pierloot, K. *Inorg. Chem.* **1991**, *30*, 2978.
(11) Chermette, H.; Bellafrouh, K,; Goursot A.; Waltz, W. L. *Chem. Phys. Lett.* **1991**, *184*, 282.
(12) Lee, S. H.; Waltz, W. L.; Demmer, D. R.; Walters, R. T. *Inorg. Chem.* **1985**, *24*, 1531.
(13) Endicott, J. F.; Ramasami, T.; Tamilarasan, R.; Lessard, R.; Ryu, C. K.; Brubaker, G. R. *Coord. Chem. Rev.* **1987**, *77*, 1.
(14) Forster, L. S. *Chem. Rev.* **1990**, *90*, 331.
(15) Kirk, A. D. *Coord. Chem. Rev.* **1981**, *39*, 225.
(16) Wilson, R. B.; Solomon, E. I. *Inorg. Chem.* **1978**, *17*, 1729.

S0020-1669(97)01520-6 CCC: $15.00
Published on Web 07/03/1998

theory holds some promise to predict the excited state distortions of transition metal complexes in order to get more insight in their photochemistry. Results within the local density approximation (LDA) and the generalized gradient approximation (GGA) will be compared with earlier reported results for $[CrX_6]^{3-}$ (X = Cl, Br).[17,18]

2. Computational Methods

2.1. Density Functional Calculations. All calculations were performed with the Amsterdam density functional (ADF) program package.[19,20] The used basis functions are those given in the program database. All atoms were described through a triple-ζ STO basis set, and the core electrons of Cr(1s−3p) and N(1s) were kept frozen. The Vosko, Wilk, and Nusair (VWN) functional[21] for exchange and correlation energies was used in the LDA calculations. In the case of the GGA calculations, we opted for the Becke−Perdew (BP) functional, which uses Becke's[22] gradient correction to the local expression of the exchange energy and Perdew's[23,24] gradient correction to the local expression of the correlation energy. The convergence criteria in the geometry optimizations, which use analytical derivatives,[25] were set to 1×10^{-3} hartree for the changes in energy, 1×10^{-3} hartree/Å for the energy gradient, 1×10^{-3} Å for the changes between old and new bond lengths, and 0.3° for changes in bond and dihedral angles.

2.2. Multiplet Structure. In the calculation of the multiplet splitting, we follow essentially the method proposed by Ziegler et al.[26] According to their results, it is possible to replace the energy of a single determinant by its corresponding statistical energy as obtained in a DF theory calculation. In general, it is not possible to express the energy of a multiplet in terms of the energy of one single determinant. However, it is possible to exploit fully the symmetry in order to simplify the relation between the multiplet splitting and the single determinantal energies. A detailed description of the symmetry reduction of the problem was recently given by Daul.[27] In general, we can write the multiplet wave function as

$$\Psi_k = |\alpha \Gamma m_\Gamma S m_S\rangle \tag{2.1}$$

where Γ and S denote the space and spin parts of the wave function, respectively, and m_Γ and m_S denote its components in case of degeneracy. The relation between multiplet energies $E(\Psi_k)$ and the energies of the nonredundant single determinants $E(\phi_{\mu j})$ is given by

$$E(\Psi_k) = \sum_{j=1} F_{kj} E(\phi_{\mu j}) \tag{2.2}$$

where the coefficients F_{kj} are the corresponding symmetry-dependent weights. This method takes only first-order (Coulombic and exchange) electrostatic interactions into account. In order to obtain the energy of single determinants in DF theory, we can follow two possible calculation schemes, as described by Daul et al.:[28] the so-called transition state (TS) method and the ΔSCF method. We will compare results obtained by both schemes. For the sake of completeness, we want to mention that there exists an alternative method for the calculation of excited states, which is based on time dependent perturbation theory.[29,30] This approach is theoretically more rigorous, but also more complex. Only very few calculations of transition energies in atoms and molecules have been reported up until now.[31−33]

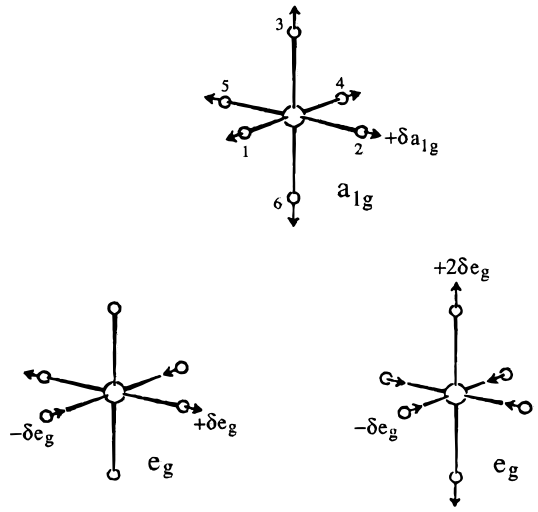

Figure 1. Symmetry-adapted displacements of the six nearest NH_3 neighbors of the chromium ion.

2.3. Frequencies. In order to determine the vibrational frequencies of $[Cr(NH_3)_6]^{3+}$ normal modes, small a_{1g} and e_g symmetry adapted displacements of the NH_3 ligands, as shown in Figure 1, around the earlier calculated equilibrium geometry were made and the corresponding total energy was calculated. The so-obtained potential energy curves were then fitted within the harmonic approximation, and frequencies ω were finally calculated as

$$\omega = \sqrt{\frac{k}{\mu_L}} \tag{2.3}$$

where k is the force constant and μ_L is the reduced mass. The normal modes Q_u can be written as

$$Q_\alpha(a_{1g}) = \sqrt{\frac{1}{6}}(\delta x_1 + \delta y_2 + \delta z_3 + \delta x_4 + \delta y_5 + \delta z_6)$$

$$Q_\mu(e_g) = \sqrt{\frac{1}{12}}(2\delta z_3 + 2\delta z_6 - \delta x_1 - \delta x_4 - \delta y_2 - \delta z_5) \tag{2.4}$$

$$Q_\nu(e_g) = \sqrt{\frac{1}{2}}(-\delta x_1 - \delta x_4 + \delta y_2 + \delta y_5)$$

where δx_L, δy_L, and δz_L are the changes of the Cartesian coordinates of ligand L (Figure 1).

3. Results and Discussion

3.1. Ground State Geometry and Frequencies. In the case of $[Cr(NH_3)_6]^{3+}$, the symmetry is not exactly octahedral, due to the presence of the NH_3 groups. A more appropriate symmetry would be D_{3d}. However, in this symmetry the main quantization axis is a 3-fold axis and second-order elements

(17) Bellafrouh, K.; Daul, C.; Güdel, H. U.; Gilardoni, F.; Weber, J. *Theor. Chim. Acta* **1995**, *91*, 215.
(18) Bellafrouh, K.; Daul, C.; Güdel, H. U.; Gilardoni, F.; Weber, J. *J. Chem. Phys.* **1996**, *104*, 7624.
(19) Baerends, E. J.; Ellis, D. E.; Ros, P. *Chem. Phys.* **1973**, *2*, 41.
(20) Baerends, E. J.; te Velde, B. *J. Comput. Phys.* **1992**, *99*, 84.
(21) Vosko, S. H.; Wilk, L.; Nusair, M. *Can. J. Phys.* **1980**, *58*, 1200.
(22) Becke, A. D. *Phys. Rev.* **1988**, *A38*, 3089.
(23) Perdew, J. P. *Phys. Rev.* **1986**, *B33*, 8822.
(24) Perdew, J. P. *Phys. Rev.* **1986**, *B34*, 7406.
(25) Versluis, L.; Ziegler, T. *J. Chem. Phys.* **1988**, *88*, 322.
(26) Ziegler, T.; Rauk, A.; Baerends, E. J. *Theor. Chim. Acta* **1977**, *43*, 261.
(27) Daul, C. *Int. J. Quantum Chem.* **1994**, *52*, 867.
(28) Daul, C. A.; Doclo, K. G.; Stükl, A. C. *Recent Advances in Density Functional Methods, Part II*; World Scientific Publishing Company: Singapore, 1997.
(29) Casida, M. E. *Recent Advances in Density Functional Methods, Part I*; World Scientific Publishing Company: Singapore, 1995.
(30) Gross, E. K. U.; Dobson, J. F.; Petrsilka, M. *Density Functional Theory II*; *Vol. 181, Topics in Current Chemistry*; Springer: Berlin, 1996.
(31) Casida, M. E.; Jamorski, C.; Casida, K. C.; Salahub, D. R. *J. Chem. Phys.* **1998**, *108*, 4439.
(32) Petersilka, M.; Gross, E. K. U. *Phys. Rev. Lett.* **1996**, *76*, 1212.
(33) Bauernschmitt, R.; Ahlrichs, R. *Chem. Phys. Lett.* **1996**, *256*, 454.
(34) Goldfield, S. A.; Raymond, K. N. *Inorg. Chem.* **1971**, *10*, 2604.
(35) Von Wieghardt, K.; Weiss, J. *Acta Crystallogr.* **1972**, *B28*, 529.
(36) Clegg, W.; Greenhalgh, D. A.; Straughan, B. P. *J. Chem. Soc., Dalton Trans.* **1975**, 2591.
(37) Clegg, W. *Acta Crystallogr.* **1976**, *B32*, 2907.

Table 1. Comparison between Experimental and Calculated Ground State Properties[a]

	VWN	BP	expt
d(Cr−N)	2.092	2.156	2.07[b]
d(N−H)	1.036	1.032	1.02[c]
angle (H−N−H)	103.7	103.9	106.6[c]
a_{1g}	337	301	462[d]
e_g	293	273	412[d]

[a] Units: Å, deg, and cm^{-1}. [b] Average value in different crystal environments.[34−37] [c] Values of the free NH_3 molecule.[38] [d] References 39−41.

(i.e., two-electron integrals which are of neither Coulombic nor exchange type) are expected to be large. In the way we calculate the multiplet splitting, these elements are not included. Thus, a more judicious choice is C_{2v}, where the main quantization axis is a tetragonal axis as in the case of octahedral symmetry. Second-order elements will be very small now. See Appendix for a more detailed discussion. In going from O_h to C_{2v} symmetry, the t_{2g} orbitals are split into a_1, a_2, and b_1, the e_g orbitals into a_1 and b_2. Due to the presence of the hydrogen atoms, the t_{2g} and e_g orbitals will not be totally degenerate. It turned out that the energy difference is very small (less than 20 cm^{-1}), so we can still handle the symmetry of the molecule as if it were exactly octahedral. For clarity, we will always make reference to the octahedral supersymmetry of the CrN_6 skeleton in the following.

The ground state of $[Cr(NH_3)_6]^{3+}$ is $^4A_{2g}$, where the three d electrons are placed in the t_{2g} shell. The energy of the $^4A_{2g}$ state can be written in terms of one single-determinantal energy, i.e., $E(^4A_{2g}) = E(|d_{yz}^+ d_{xz}^+ d_{xy}^+|)$. The geometry was optimized in two steps:

1. Let the Cr−N distance relax, keeping the N−H distance and the H−N−H angle fixed.

2. Starting from the geometry obtained in step 1, let the N−H distance and the H−N−H angle relax, keeping the Cr−N distance fixed.

The results obtained in this way are listed in Table 1, together with the calculated a_{1g} and e_g frequencies. The theoretical N−H distance and the angle H−N−H are compared with the experimental values for the free NH_3 molecule. It is well-known that X-ray diffraction yields X−H (X = N, C, O) distances that are too low.[38] In this light, the results obtained in our calculations can be considered as very reasonable. However, the most important geometrical parameter is the Cr−N bond length. As can be seen from Table 1, the experimental value is overestimated by 0.022 Å when a local functional is used and by 0.086 Å when a gradient corrected (GC) functional is used. A similar observation was made by Bray et al.[42] in a series of 17 classical Werner-type transition metal complexes: LDA tends to give bond lengths which are in average 0.02 Å too long whereas GGA gives an averaged elongation of about 0.07 Å. These authors pointed out that the source of the error is unclear, but they made a correlation between the magnitude of the expansion and the covalency: the smaller the covalent character of the bond, the larger the expansion induced by a GGA calculation. In order to check this statement, a comparison between $[CrCl_6]^{3-}$, $[Cr(NH_3)_6]^{3+}$, and $[CrF_6]^{3-}$ is given in Table 2. The covalency of a bond can be related with the *nephelauxetic effect*,[46,47] which states that a transfer of electronic charge from the ligands to the central metal ion causes an expansion of the metal d orbitals, which lowers the d−d repulsion energy. Corresponding to the empirical *nephelauxetic series*,[46,47] we can thus say that the Cr−Cl bond is more covalent than the Cr−NH_3 bond, which is in turn more covalent than the Cr−F bond. Following Bray et al.,[42] we should then observe the largest deviation of the metal−ligand distance for the $[CrF_6]^{3-}$ complex. As can be seen from Table 2, this is indeed the case. It has to be pointed out that, in all of these calculations, lattice effects are not taken into account. As shown by Gilardoni et al.,[18] the inclusion of the Madelung potential shifts the values for the bond lengths in the right direction, but the magnitudes of the shifts are insufficient to bring the values into line with the experimental ones. In the case of the $[CrF_6]^{3-}$ complex,[44] it was even necessary to include the first and second neighbors explicitly in order to obtain a good description of the Cr−F bond length. The inclusion of the Madelung potential is not a trivial matter, certainly not if one deals with lower symmetry lattices, as is the case in this study. Therefore, we decided to perform all calculations on the isolated $[Cr(NH_3)_6]^{3+}$ complex. The slight discrepancy in the structure should not modify significantly the prediction of the photophysical properties.

Table 2. Comparison between Experimental and Calculated Metal−Ligand Distances,[a] Using the BP Functional

	BP	expt
d(Cr−Cl) in $[CrCl_6]^{3-}$	2.481[b]	2.44[c]
d(Cr−N) in $[Cr(NH_3)_6]^{3+}$	2.156	2.07[d]
d(Cr−F) in $[CrF_6]^{3-}$	2.018[e]	1.88[f]

[a] Units: Å. [b] Reference 17. [c] Reference 43. [d] Average value in different crystal environments.[21−24] [e] Reference 44. [f] Reference 45.

The calculated vibrational frequencies are too low in comparison with experiment, as is also the case[18] for $[CrCl_6]^{3-}$ and $[CrBr_6]^{3-}$. A similar observation was made in a set of organic molecules by Johnson et al.,[48] but the discrepancies with experiment in the case of transition metal complexes turn out to be larger. However, the relative positions of the frequencies of the a_{1g} and e_g normal modes are reproduced by our calculations.

3.2. Excited State Properties. In the absorption spectrum of $[Cr(NH_3)_6]^{3+}$, one observes two broad spin-allowed quartet−quartet bands, assigned to the following transitions: $^4A_{2g} \rightarrow {}^4T_{2g}$ and $^4A_{2g} \rightarrow {}^4T_{1g}$. These two transitions arise from a single excitation from the t_{2g} shell to the e_g shell. The spin-forbidden intraconfigurational transition $^4A_{2g} \rightarrow {}^2E_g$ is observed at lower energy. The two other intraconfigurational transitions, i.e., $^4A_{2g} \rightarrow {}^2T_{1g}$ and $^4A_{2g} \rightarrow {}^2T_{2g}$, are not observed, but a good estimation of their values can be made by comparison with the absorption spectrum of a similar complex, like $[(+)_D\text{-}Cr(en)_3]^{3+}$.[49] In doing so, we can see that the transition to $^2T_{1g}$ would be found

(38) Hamilton, W. C.; Ibers, J. A. *Hydrogen Bonding in Solids*; Benjamin: New York, 1968.
(39) Siebert, H.; Eysel, H. *J. Mol. Struct.* **1969**, *4*, 29.
(40) Schmidt, K. H.; Müller, A. *Inorg. Chem.* **1975**, *14*, 2183.
(41) Nakamoto, K. *Infrared Spectra of Inorganic and Coordination Compounds*; Wiley: New York, 1971.
(42) Bray, M. R.; Deeth, R. J.; Paget, V. J.; Sheen, P. D. *Int. J. Quantum Chem.* **1996**, *61*, 85.
(43) Reber, C.; Güdel, H. U.; Meyer, G.; Schleid, T.; Daul, C. *Inorg. Chem.* **1989**, *28*, 3249.
(44) Aramburu, A.; Moreno, M.; Doclo, K.; Daul, C. Unpublished results.
(45) de Lucas, M.; Dance, J. M.; Rodriguez, F.; Tressaud, A.; Moreno, M. *Radiat. Eff. Defects Solids* **1995**, *135*, 517.
(46) Jörgenson, C. K. *Modern Aspects of Ligand Field Theory*; North-Holland Publishing Company: Amsterdam, 1971.
(47) Gerloch, M.; Slade, R. C. *Ligand-Field Parameters*; Cambridge University Press: Cambridge, England, 1973.
(48) Johnson, B.; Gill, P. M. W.; Pople, J. A. *J. Chem. Phys.* **1993**, *98*, 5612.
(49) Geiser, U.; Güdel, H. U. *Inorg. Chem.* **1981**, *20*, 3013.
(50) Zinato, E.; Lindholm, R.; Adamson, A. W. *J. Inorg. Nucl. Chem.* **1969**, *31*, 229.

Table 3. Comparison between Experimental and Calculated Ligand Field Transitions Obtained by the ΔSCF and the TS Procedure, Using the Optimized Geometry

	VWN		BP	
	TS	ΔSCF	ΔSCF	expt
$^4A_{2g} \rightarrow {}^2E_g$	12 243	12 233	11 966	15 267[b]
$^4A_{2g} \rightarrow {}^2T_{1g}$	14 790	14 223	16 056	15 900[c]
$^4A_{2g} \rightarrow {}^2T_{2g}$	29 252	22 378	24 033	21 600[c]
$^4A_{2g} \rightarrow {}^4T_{2g}$	24 975	25 228	22 711	21 552[d]
$^4A_{2g} \rightarrow {}^4T_{1g}$	31 406	31 614	30 283	28 409[d]

[a] Units: cm^{-1}. [b] Reference 50. [c] Estimated value. [d] Reference 13.

about 600 cm^{-1} higher than the ^2E_g band and that the transition to $^2T_{2g}$ would be observed on top of the $^4T_{2g}$ band.

The energies of all calculated multiplets can be obtained to first order, as shown below, from the energies of five nonredundant single determinants,

$$E(^4A_{2g}) = E(|\xi^+\eta^+\xi^+|)$$

$$E(^4T_{2g}) = E(|\mu^+\xi^+\eta^+|)$$

$$E(^4T_{1g}) = E(|\nu^+\xi^+\eta^+|)$$

$$E(^2E_g) = 1.5E(|\xi^+\eta^-\xi^-|) - 0.5E(|\xi^+\eta^+\zeta^+|) \quad (3.1)$$

$$E(^2T_{1g}) = E(|\xi^-\eta^+\eta^-|) + 0.5E(|\xi^+\eta^+\zeta^+|) - 0.5E(|\xi^+\eta^-\zeta^-|)$$

$$E(^2T_{2g}) = E(|\xi^-\eta^+\eta^-|) + 0.5E(|\xi^+\eta^+\zeta^+|) + 0.5E(|\xi^+\eta^-\zeta^-|)$$

where μ and ν are the components of e_g (d_{z^2} and $d_{x^2-y^2}$, respectively) and ξ, η- and ζ the components of t_{2g} (d_{yz}, d_{xz}, and d_{xy}, respectively). The energies thus obtained can be found in Table 3. The calculated absorption maxima for the spin-allowed Franck−Condon transition of $^4A_{2g} \rightarrow {}^4T_{2g}$ and $^4A_{2g} \rightarrow {}^4T_{1g}$ are about 3000 cm^{-1} too high when the simple LDA is used, whereas these values are only about 1500 cm^{-1} too high when the more elaborate GGA is used. Concerning the spin-forbidden transitions, the values are roughly 3000 cm^{-1} too low for ^2E_g, in agreement with experiment for $^2T_{1g}$, and 2000 cm^{-1} too high for $^2T_{2g}$. The best results are in all cases obtained with the BP functional; GC functionals are indeed designed to give better energetics. A similar accuracy was observed when the d−d excitation energies of $[CrX_6]^{3-}$ (X = Cl, Br) were calculated.[17,18]

From inspection of Table 3, it can also be seen that good agreement is obtained for the two different calculation schemes, i.e., the ΔSCF and the TS procedure. This is in line with the earlier findings of Stückl et al.[51] Both procedures take into account the energetic (exchange) effect due to the unpaired spins, but the orbital relaxation effects, due to a different occupation of spin orbitals with the same space but different spin parts, are neglected. An improvement of the method would consist of letting the orbitals relax during the calculation of the single determinants. This has only a physical meaning when the multiplets can be represented by one single determinant.

Table 4. Comparison between Experimental and Calculated Distortion Properties of the $^4T_{2g}$ State[a]

	VWN	BP	expt[b]
Δ[Cr−N(*x*,*y*)]	+0.143	+0.149	+0.12
Δ[Cr−N(*z*)]	−0.022	−0.031	−0.02
Jahn−Teller energy	1164	1077	920
a_{1g}	308	277	403
e_g	267	243	403

[a] Units: Å and cm^{-1}. [b] Reference 16.

Hence, we calculated in this way the two quartet−quartet transitions, using the BP functional. This results in an energy of 22 369 cm^{-1} for $^4T_{2g}$ and 28 780 cm^{-1} for $^4T_{1g}$, which is in excellent agreement with experiment!

$^4T_{2g}$ derives from the $(t_{2g})^2(e_g)$ electron configuration in first order. As the e_g orbital is more antibonding than the t_{2g} orbital, one expects a larger equilibrium Cr−N distance in the $^4T_{2g}$ state than in the $^4A_{2g}$ ground state. This is indeed reflected in our calculations: the minimum of the $^4T_{2g}$ potential energy curve is located at a Cr−N distance, which is 0.086 Å longer relative to the $^4A_{2g}$ equilibrium distance when the VWN functional is used and 0.088 Å longer when the BP functional is used. We also calculated the energy of the excited ^2E_g state as a function of the bond length. The value of this state lies independently of the bond length about 12 000 cm^{-1} above the $^4A_{2g}$, showing that the potential energy curves of the $^4A_{2g}$ and the ^2E_g state have a similar form. Experimentally, this is reflected in the narrow bands in absorption and emission spectra and the very small Stokes shift.

The vibrations of the a_{1g} and e_g normal modes for the $^4T_{2g}$ state are calculated lower than the experimental values; see Table 4. This was also the case for the ground state. However, it is confirmed that the frequencies are somewhat decreased in the $^4T_{2g}$ state, as observed experimentally.[16] An e_g Jahn−Teller distortion is reported[16] in the thermally equilibrated $^4T_{2g}$ state, as expected from the orbital degeneracy of this state. Figure 2 displays the contour levels of $^4T_{2g}$ as a function of the axial *d*(Cr−N(*z*)) and the equatorial *d*(Cr−N(*x*,*y*)) bond lengths. The system moves to a more stable geometry when the axial bonds are compressed and the equatorial ones are elongated. The experimental Jahn−Teller energy can be calculated as $E_{JT} = S_{eg}\hbar\omega_{eg}$, with the values for S_{eg} and ω_{eg} taken from the paper of Solomon et al.[16] The calculated energy gain and the geometry changes, relative to the calculated ground state geometry, are in very good agreement with experiment; see Table 4. This confirms the results obtained for $[CrX_6]^{3-}$ (X = Cl, Br).[17,18] As stated there, the fact that DF theory can reproduce the consequences of a Jahn−Teller coupling in the excited state, is very important because only in very few cases can such information be obtained experimentally.

Another feature that we can predict from the obtained minimum in the energy of the $^4T_{2g}$ state is the 0−0 energy gap between this state and the ^2E_g state, which represents the minimum energy required for a bisc process. This value is not known experimentally, because no prompt or delayed fluorescence from the $^4T_{2g}$ state is observed. Following the thought of Fleischauer et al.,[52] this value can be estimated to be 4400 cm^{-1}. The BP calculation predicts a value of 6390 cm^{-1}. However, as we can predict the d−d excitation energies only with an accuracy of roughly 2000 cm^{-1}, care should be taken in interpreting this result.

(51) Stückl, A. C.; Daul, C. A.; Güdel, H. U. *Int. J. Quantum Chem.* **1997**, *61*, 579.

(52) Fleischauer, P. D.; Adamson, A. W.; Sartori, G. *Prog. Inorg. Chem.* **1972**, *17*, 1.

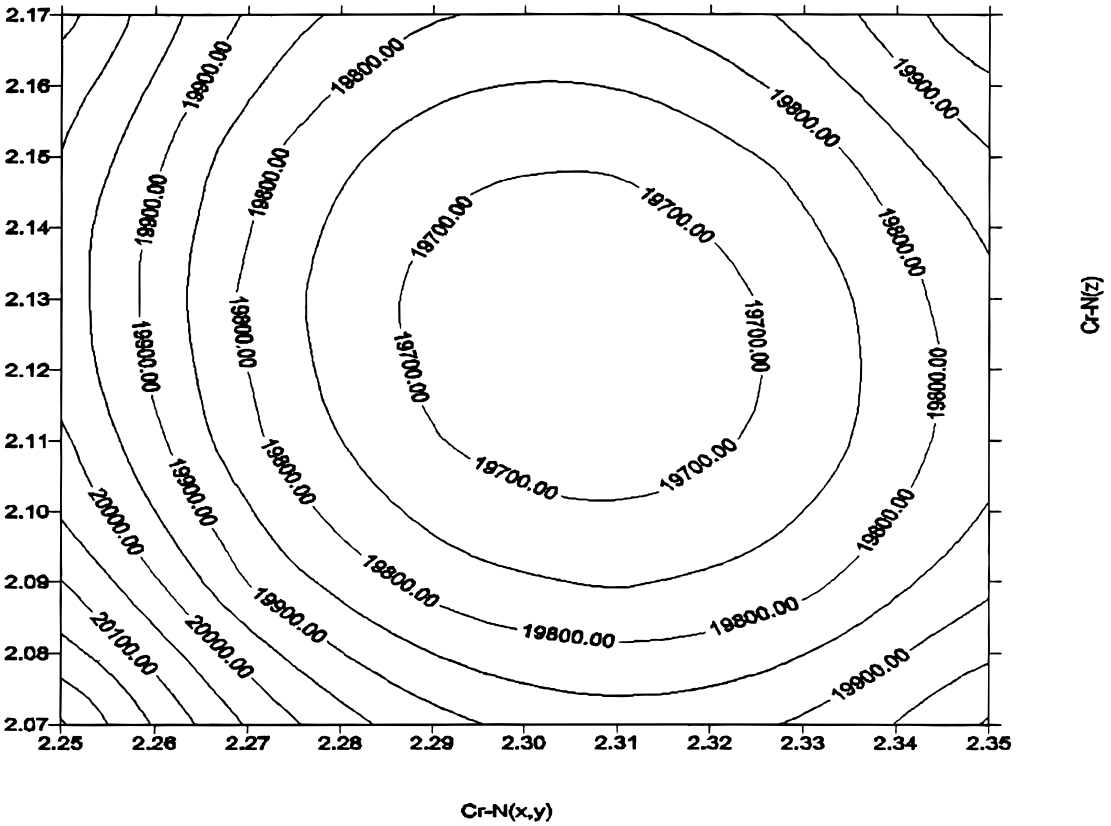

Figure 2. Contour levels of the $^4T_{2g}$ potential energy surface, calculated as a function of both Cr−N(x,y) and Cr−N(z) distances, using the BP functional (energies in cm^{-1}).

4. Conclusions

It has been found that the ground state geometry of $[Cr(NH_3)_6]^{3+}$ is well described in the LDA. The GGA calculations tend to lengthen the Cr−N bond too much. An improvement of these results can certainly be obtained by including the Madelung potential or by making calculations on a bigger cluster. However, the relative geometry changes of the Jahn−Teller active $^4T_{2g}$ state are reproduced by both classes of functionals. The d−d excitation energies are best described with the BP functional. When orbital relaxation is taken into account, quartet−quartet transition energies are in perfect agreement with experiment. Thus, the results of DF calculations have a certain predictive character and can be a helpful tool in gaining more insight in the photophysics and photochemistry of transition metal complexes.

Acknowledgment. This work was supported by the Swiss National Science Foundation.

Appendix

As described in detail in a former publication,[27] the method used to calculate the multiplets includes only the first-order interactions. This has as the important consequence that the results are dependent on the choice of the axes. In order to illustrate this point, we consider in the following the formal results of a simple ligand field approach. For the sake of clarity, we have omitted always the subscripts for gerade and ungerade.

In octahedral symmetry, the $(t_2)^3$ and $(t_2)^2(e)^1$ configurations give rise to three quartets, i.e., $^4A_2$, $^4T_2$, and $^4T_1$. Their corresponding energies are 0, Δ, and $\Delta + 12B$, respectively.

Table A.1. Electrostatic Matrix Elements Expressed in Terms of Racah Parameters in D_{3d} Symmetry

^4E	$(1e)^2\ [^3A_2]\ (2e)$	$(1e)\ (1a_1)\ [^3E]\ (2e)$
$(1e)^2\ [^3A_2]\ (2e)$	$3A - 9B + \Delta$	$-6B$
$(1e)\ (1a_1)\ [^3E]\ (2e)$	$-6B$	$3A - 9B + \Delta$
$^4A_2$	$(1e)^2\ [^3A_2]\ (1a_1)$	$(1e)^2\ [^3E]\ (2e)$
$(1e)^2\ [^3A_2]\ (1a_1)$	$3A - 15B + \Delta$	0
$(1e)^2\ [^3E]\ (2e)$	0	$3A - 3B + \Delta$
$(1e)^2\ [^3E]\ (2e)$	$^4A_1 = 3A - 15B + \Delta$	

Let us have a look now how these multiplets behave in D_3 and C_{2v}, both subgroups of the octahedral group. Descending in symmetry to the D_3 and C_{2v} groups yields the following correlation table for the irreducible representations:

O	D_3	C_{2v}
$1t_{2(\xi)}$	$1e(\epsilon)$	$1b_2$
$1t_{2(\eta)}$	$1e(\theta)$	$1b_1$
$1t_{2(\zeta)}$	$1a_1$	$1a_2$
$1e(\epsilon)$	$2e(\epsilon)$	$1a_1$
$1e(\theta)$	$2e(\theta)$	$2a_1$

In D_3 symmetry the ground and singly excited quartet states become

$$^4A_2 \rightarrow {}^4A_2$$

$$^4T_2 \rightarrow {}^4E + {}^4A_1$$

$$^4T_1 \rightarrow {}^4E + {}^4A_2$$

The electrostatic matrix elements for the ground and singly excited quartet states of the d^3 ligand field configuration are

Table A.2. Energies of the Different Quartet States in the D_3 Symmetry

	first order	first + second order
$(1e)^2\,(1a_1)\,{}^4A_2$	0	0
$(1e)\,(1a_1)\,(2e)\,{}^4A_1$	Δ	Δ
$(1e)\,(1a_1)\,(2e)\,{}^4E$	$\Delta + 6B$	Δ
$(1e)\,(1a_1)\,(2e)\,{}^4A_2$	$\Delta + 12B$	$\Delta + 12B$
$(1e)\,(1a_1)\,(2e)\,{}^4E$	$\Delta + 6B$	$\Delta + 12B$

given in Table A.1. Now, it is possible to calculate the multiplet energies within the ligand field approximation including only first- or including first- and second-order electrostatic interactions. The results are depicted in Table A.2. It is immediately clear that the inclusion of the second-order electrostatic interactions is necessary to obtain the correct the result.

The situation is clearly different in C_{2v} symmetry; here the ground and singly excited quartet states become

$$^4A_2 \rightarrow {}^4A_1$$

$$^4T_2 \rightarrow {}^4A_2 + {}^4B_1 + {}^4B_2$$

$$^4T_1 \rightarrow {}^4A_2 + {}^4B_1 + {}^4B_2$$

As the system of axes is the same for the octahedral group, there are no second-order electrostatic interactions and one obtains already in the first-order approximation the correct results (cf. Table A3). At this point, it is important to notice that there is no way to express the second-order electrostatic elements in the D_3 symmetry in terms of single determinantal energies. A way around this problem consists of calculating explicitly the second-order electrostatic elements from the appropriate SCF wave function, as already suggested by Cook et al.[53] As this approach is theoretically not very well founded, it should be handled with care. Another possibility to obtain in D_3 symmetry the energies of the two single excited quartet states is to calculate to first order the energies of $^4A_2$ [$(1e)^2$-(2e)] and $^4A_1$ [$(1e)^2(2e)$]. However, in this case, the calculation of more single determinants is needed. For these reasons, it is clear that the latter symmetry group is the best choice to tackle the multiplet problem.

Table A.3. Energies of the Different Quartet States in the C_{2v} Symmetry

	first order	first + second order
$(1a_2)\,(1b_1)\,(1b_2)\,{}^4A_1$	0	0
$(1a_2)\,(1b_1)\,(1a_1)\,{}^4B_2$	Δ	Δ
$(1a_2)\,(1b_2)\,(1a_1)\,{}^4B_1$	Δ	Δ
$(1b_2)\,(1b_1)\,(1a_1)\,{}^4A_2$	Δ	Δ
$(1a_2)\,(1b_1)\,(2a_1)\,{}^4B_2$	$\Delta + 12B$	$\Delta + 12B$
$(1a_2)\,(1b_2)\,(2a_1)\,{}^4B_1$	$\Delta + 12B$	$\Delta + 12B$
$(1b_2)\,(1b_1)\,(2a_1)\,{}^4A_2$	$\Delta + 12B$	$\Delta + 12B$

IC9715207

(53) Cook, M.; Karplus, M. *Chem. Phys. Lett.* **1981**, *84*, 565.